Magnetic coupling between nonmagnetic ions: Eu^{3+} in EuN and EuP

M. D. Johannes[1] and W. E. Pickett[2]
[1]*Code 6391, Naval Research Laboratory, Washington, D.C. 20375, USA*
[2]*Department of Physics, University of California Davis, Davis, California 95616, USA*
(Received 9 August 2005; published 28 November 2005)

We consider the electronic structure of, and magnetic exchange (spin) interactions between, nominally nonmagnetic Eu^{3+} ions ($4f^6$, $S=3$, $L=3$, $J=0$) within the context of the rocksalt structure compounds EuN and EuP. Both compounds are ionic (Eu^{3+}; N^{3-} and P^{3-}) semimetals similar to isovalent GdN. Treating the spin polarization within the $4f$ shell, and then averaging consistent with the $J=0$ configuration, we estimate semimetallic band overlaps (Eu $5d$ with pnictide $2p$ or $3p$) of $\sim$0.1 eV (EuN) and $\sim$1.0 eV (EuP) that increase (become more metallic) with pressure. The calculated bulk modulus is 130 (86) GPa for EuN (EuP). Exchange (spin-spin) coupling calculated from correlated band theory is small and ferromagnetic in sign for EuN, increasing in magnitude with pressure. Conversely, the exchange coupling is antiferromagnetic in sign for EuP and is larger in magnitude, but decreases with compression. Study of a two-site model with $\vec{S}_1 \cdot \vec{S}_2$ coupling within the $J=0,1$ spaces of each ion illustrates the dependence of the magnetic correlation functions on the model parameters, and indicates that the spin coupling is sufficient to alter the Van Vleck susceptibility. We outline a scenario of a spin-correlation transition in a lattice of $S=3$, $L=3$, $J=0$ nonmagnetic ions.

DOI: 10.1103/PhysRevB.72.195116 PACS number(s): 71.10.−w, 71.20.Eh

I. INTRODUCTION

The readily observable behavior of the angular momentum and associated magnetic moment of rare-earth ions is one of the more obvious successes of the quantum-mechanical description of atomic magnetism. Hund's rules for the total angular momentum $\vec{J}=\vec{L}+\vec{S}$ in terms of orbital filling (giving orbital L and spin S angular momenta) are simple and successful. The most striking prediction is when the angular momenta in a spin polarized $S\neq 0$ and orbitally polarized $L\neq 0$ ion conspire to give a nonmagnetic ground state $J=0$. The canonical example is $Eu^{3+} f^6$: $S=3$, $L=3$, $J=0$. Whereas Eu^{3+} is nonmagnetic experimentally (unresponsive to magnetic fields, treatment of the high spin polarization $\vec{S}^2=12$ (we use $\hbar=1$) is essential for obtaining any reasonable model of the electronic structure.

The orbital polarization and associated moment $\vec{m}_L=\mu_B\vec{L}$ is a secondary effect as far as the determination of the electronic structure is concerned, because the magnetic coupling proceeds via the influence of the spin moment $\vec{m}_S=2\mu_B\vec{S}$ on the electronic structure and on neighboring spins (via exchange coupling). $\vec{L}$ is however central in determining $\vec{J}$ and the total moment, which for Eu^{3+} is large: $|\vec{M}|=\mu_B|(\vec{L}+2\vec{S})| = \mu_B|(\vec{J}+\vec{S})|=\mu_B|\vec{S}|\approx 3.5\mu_B(\langle\vec{M}^2\rangle_{J=0}=12\mu_B^2)$. Of course, in the $J=0$ ground state the moment has zero projection along any axis including any applied field, hence the "nonmagnetic" character of the ion. These considerations do not change the fact that the ion has a large intrinsic spin polarization, and that there will be exchange (spin-spin) coupling between neighboring spins; $\langle\vec{S}_i\rangle=0$ does not imply $\langle\vec{S}_i\cdot\vec{S}_j\rangle =0$. Such coupling may be difficult to observe because the most direct means of observing magnetic coupling is via response to a magnetic field.

In this paper we address some of the questions raised by the interaction between these strongly polarized yet nonmagnetic ions within the context of two of the simplest solid state realizations, the binary compounds EuN and EuP. EuN is a semimetal with a simple rocksalt structure. Although it has been known for fifty years, there is little characterization of this compound in the literature. Reported values of the lattice constant are consistent at 5.020 ± 0.006 Å.[1–4] Only a very small non-stoichiometry range exists, although magnetic Eu^{2+} impurities can occur in sufficient concentration in some samples to mask the susceptibility of the Eu^{3+} ion in EuN.[5] There is also sparse literature for EuP, a compound both isostructural and isovalent to EuN. The lattice constant of EuP is measured[6] to be 5.756 Å. The 15% increase in lattice constant (50% larger volume) compared to EuN has a significant effect on the exchange interaction, probably by shifting the balance between competing mechanisms of exchange coupling.

Although any projection $\langle\vec{S}_i\rangle$ vanishes, when two neighboring ions are coupled the spin-spin *correlation* $\langle\vec{S}_1\cdot\vec{S}_2\rangle$ should be nonzero. Correspondingly there will be a term in the microscopic Hamiltonian (i.e., an energy) $K\Sigma_{\langle ij\rangle}\vec{S}_i\cdot\vec{S}_j$ for all interacting pairs. (We denote the exchange coupling by K and retain J for other uses.) This coupling in itself breaks the spherical symmetry of the ion, coupling the $J=0,1,2,\ldots,L+S$ states and allowing magnetic behavior to emerge. This effect is already seen in the magnetic susceptibility of the Eu^{3+} ion, where the magnetic field breaks the spherical symmetry, mixes $J=1$ with $J=0$ character, and gives rise to the van Vleck susceptibility.[7–10]

One may consider then whether this exchange coupling results in a phase transition; that is, a coupling strength or temperature for which the spin correlation length diverges. If the $J=0$ state of each ion is predominant, there will be only a weak magnetic signal and also minor magnetic entropy $[k_B\ln(2J+1)\rightarrow 0]$; this is the observed nonmagnetic behavior of the Eu^{3+} solid. Vanishing entropy implies that ordering

could not be seen thermodynamically; on the other hand, with free energy devoid of magnetic entropy, ordering could occur at much higher temperatures. Neutron scattering, which has sensitivity to the difference between spin and orbital moments, should be able to detect long range antialigned ordering of the spins (hence of the magnetic moments) because of the antiferromagnetic (AFM) Bragg peak. This (still primarily $J=0$) lattice of ions may therefore show a new kind of phase transition in which the $\langle \vec{S}_i \cdot \vec{S}_j \rangle$ correlation length diverges but with small (perhaps negligible) decrease in entropy.

One can avoid the entropic issues by considering the system at zero temperature. As the $J=1$ state gets mixed in, by exchange coupling and by crystalline anisotropy: how will magnetic behavior evolve and assert itself? and if there is a quantum phase transition, how would it assert itself? This process can be controlled, and ordering tendencies enhanced, at either zero or nonzero temperature, by pressure-induced volume reduction.

In this paper we begin to pursue this line of reasoning quantitatively. We first apply density functional based correlated band theory (LDA+U) to study the electronic structures of EuN and EuP and their equations of state. In the process we investigate the extent to which correlated LDA +U results can reproduce Hund's rules (more specifically, the z components of the angular momenta). We then apply conventional procedures to express the coupling in terms of a Heisenberg exchange coupling constant K between nearest neighbors. Using this exchange coupling, the known spin-orbit coupling (SOC) constant, and a single-ion anisotropy parameter, we look at a toy model of coupled ions, each of which has the $S=3$, $L=3$, $J=0$ ground state of Eu^{3+}. Specifically, we consider whether spin-spin correlations between these "$J=0$ ions" can be detected, which has some bearing on the question of a phase transition (divergent correlation length). The difficult questions of addressing a *bona fide* phase transition are, unfortunately, beyond the scope of this paper.

II. CALCULATIONAL METHODS

For Eu as for most rare-earth ions it is necessary to use the LDA+U method (or another orbital-functional approach) to separate the occupied $4f$ orbitals from the unoccupied ones, because LDA invariably results incorrectly in narrow partially filled $4f$ bands straddling the Fermi level. For our LDA+U calculations, we have chosen a value $U=8$ eV for the effective Coulomb repulsion and a value of $J^H=1$ eV for the intra-atomic $4f$ exchange interaction on the Eu ion. These values were chosen by comparison with other Eu compounds.[11,12] Since U is so large, the specific value of U should not substantially change the conclusions about magnetic coupling which are obtained. The value of J^H is typical of what is used for rare-earth ions, and the effects of changing it have been found to be small. The nonintuitive effect on the electronic structure of the "exchange" J^H as it arises in the LDA+U method will be discussed in a Sec. III C.

All band structure calculations were performed using the program[13] WIEN2K, which employs an APW+LO (augmented plane wave plus local orbitals) basis set. This allows for a lower plane wave cutoff than is necessary for LAPW calculations, and consequently the RK_{max} was set to 7.00. We used the LDA exchange-correlation parameterization of Perdew and Wang[14] and added a Hubbard U according to the prescription of Anisimov *et al.*[15,16] In this scheme, the double counting terms are subtracted assuming a fully localized (i.e., atomic) limit.[17] Details of the implementation of the LDA +U method into the LAPW code can be found in the full description of Shick *et al.*[18]

Band structure methods are seriously limited in the treatment of rare earth ions due to their classical treatment of the spin and orbital angular momentum (and for other reasons). As usual, we assign a direction (local z axis) to $\vec{S},\vec{L}$ and deal explicitly with only the corresponding projections S_z,L_z; one might say that we go into the reference frame of the spin on one Eu ion. The closest approximation to the $J=0$ state is then $S_z=3$, $L_z=-3$, which uniquely specifies the occupation of one-electron $4f$ orbitals. In an open-shell rare-earth ion, Hund's coupling first determines the total spin, S, and then the total angular momentum L. The final step is the coupling of S to L through the spin-orbit interaction. In our effective single particle picture, however, the only choice is to couple S and L at the one-electron level, which is at least partially incorrect. One could imagine neglecting the single particle spin-orbit term, choosing instead to enforce the proper relationship between spin and orbital moments by hand, perhaps by manipulating the density matrix within the LDA+U framework. But, without any spin-orbit interaction, the L_z and $-L_z$ states give rise to the same density, and hence will be degenerate. Unless the related symmetry is broken, they will be equally occupied with a resulting overall orbital moment of zero, which is clearly incorrect. We therefore moderate the failings of both methods by using a combination of the two. We include a single-particle spin-orbit interaction, using a fully relativistic approach for the core electrons and a second variational method for the valence states. Additionally, we weight the initial density matrices such that the total orbital moment projected along a chosen z axis is antiparallel to the total spin moment projected along the same axis. For this axis, we chose the cubic (111) direction, both in the doubled (rhombohedral) and single (cubic) symmetries.

Crystal field effects in both EuN and EuP are likely overestimated by the LDA, resulting in an orbital moment that is "overquenched." Comparing energies of the $S_z=3$, $L_z=-3$ state and a mixed state with a diminished orbital moment of $L_z=-1.5$, we find an energy difference of about 25 mRy for both EuN and for EuP. The $J_z=0$ state *is* (meta)stable and at some volumes the system converges preferentially to this state, despite its somewhat higher total energy. Such energy differences in LDA+U sometimes seem to approximate excitations of the $4f$ shell.[19] For these Eu pnictides and at the current level of understanding, these energy differences should probably not be taken too seriously; furthermore, the only noticeable changes in the band structure between the two orbital configurations occur in the splittings between occupied $4f$ states (see Sec. III C). We therefore use the lower-energy state in our interpretations, keeping in mind that, in reality, the orbital moment is likely to be larger than our calculated moment.

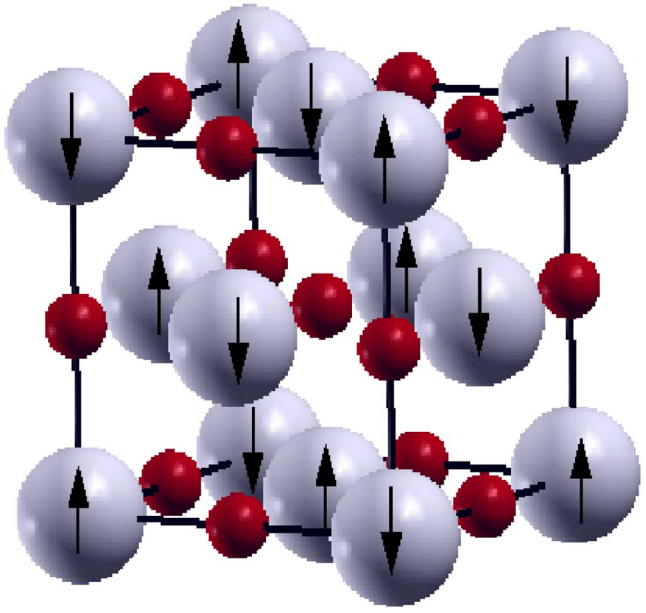

FIG. 1. (Color online) The AFMII spin ordering of a rocksalt structure compound, such as is common in the transition metal monoxides. All second nearest neighbor spins, which are coupled by the 180° superexchange coupling, are antialigned in this ordered phase.

It is unclear from the outset whether the exchange coupling will favor alignment (ferromagnetism FM) or antialignment, AFMII, for example. (We use FM and AFM to refer to the relative spin alignment in our calculations.) While the great majority of magnetic insulators are AFM, in particular the transition metal monoxides, the rocksalt structure EuO and Eu chalcogenides are FM or become FM under pressure.[12] In the calculations we present, we double the unit cell to investigate the energetics of AFMII ordering (see Fig. 1). To obtain an AFM solution, AFM symmetry of the wave functions and of the LDA+U occupation matrix has been imposed. Occasionally the AFM symmetry constraint was released to ensure that the solution remains stable without constraint.

III. ELECTRONIC STRUCTURE

A. EuN

As mentioned above, LDA is qualitatively incorrect for the localized $4f$ states of EuN, and LDA+U must be used to separate occupied from unoccupied $4f$ states. In Fig. 2, the LDA and LDA+U band structure results for the majority bands of FM EuN are displayed. The LDA results are qualitatively incorrect and will not be discussed. The N $2p$ bands lie in the range −4 to 0 eV. The lower conduction bands are of Eu $5d$ character, disrupted by the single empty majority spin f band, and overlap the N $2p$ bands at the X point of the zone to form a semimetallic band structure. The $f^6S=3$ configuration is represented by six flat $4f$ bands in the −4.5 to −7 eV range separated roughly by U from the single unoccupied majority $4f$ state lying 1 eV above E_F. The $4f$ bands are so localized that they do not overlap even with neighboring $4f$ orbitals, making direct exchange negligible. As we will show, the Eu $5d$ states are considerably extended and provide one mechanism for coupling of the localized spins (and hence the moments) on the Eu ions.

The effects of the spin polarization of the localized $4f^6$ shell on the electronic structure are considerable and nonintuitive. Via the on-site Hund's coupling (contained in the LDA exchange potential) the Eu $5d$ bands are polarized with the same orientation, with an exchange splitting of 0.6 eV. The N $2p$ bands are also polarized, but in the opposite direction. As a result, the majority $2p$ bands lie *above* the minority bands, and the induced magnetization on N is negative. While the majority Eu $5d$ band overlaps the majority $2p$ band at E_F, there is a gap between the respective minority bands. Hence FM EuN is half metallic within conventional LDA+U band theory.

A comparison of the FM band structure of EuN in a compressed face-centered cubic (fcc) unit cell and the AFM band structure in a similarly compressed, doubled, rhombohedral unit cell is shown in Fig. 3. Compression moves the Eu $5d$ bands down relative to the N $2p$ bands, increasing the filling of $5d$ states at the X point (L in the rhombohedral cell) and beginning to fill a minority Eu $5d$ pocket. Thus half metallicity is lost under moderate compression (pressure). The

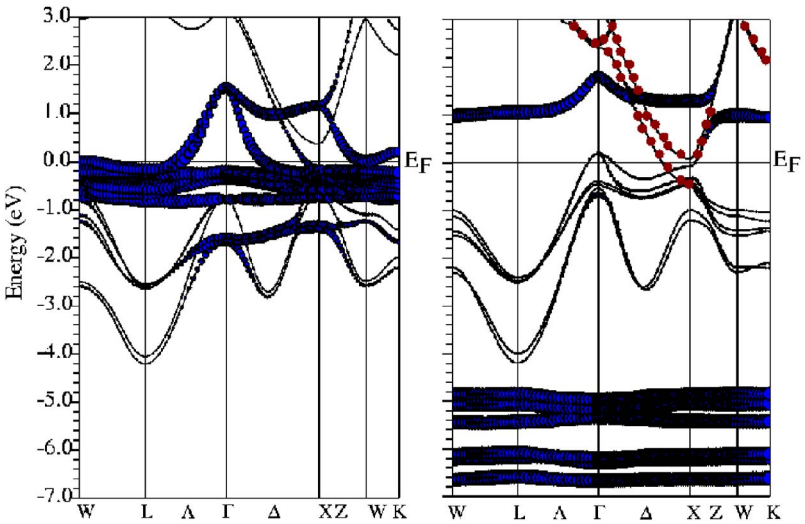

FIG. 2. (Color online) Band structures of EuN in the simple unit cell with the $4f$ character highlighted by broadened symbols. Left panel: the incorrect metallic solution given by LDA. Right panel: The LDA+U solution has six filled majority $4f$ bands and a single empty $4f$ majority spin band, separated roughly by the value of U. The occupied $4f$ band splittings (heavy lines) are discussed in the text. The Eu $5d$ conduction band dips below the Fermi energy to cross the valence N p bands at the X point; Eu $5d$ character is denoted by the (red) circles.

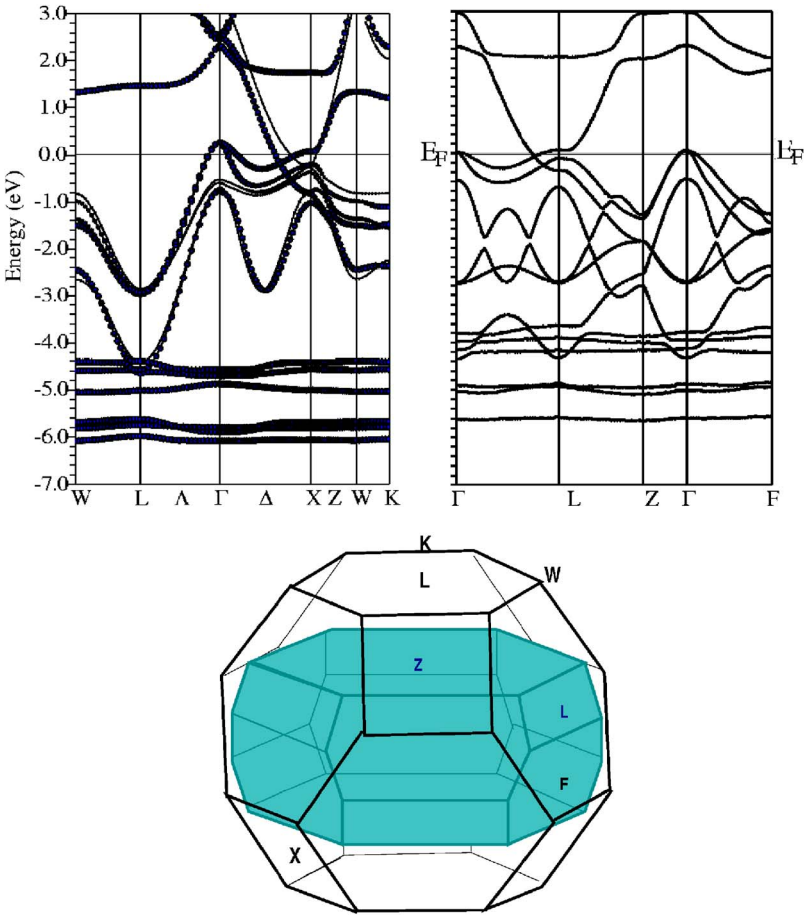

FIG. 3. (Color online) A direct comparison of EuN FM and AFM band structures at a 4% compressed lattice constant (15 GPa pressure). The FM configuration (left) is shown in the FCC unit cell with all majority spin states highlighted, while the AFM configuration (right) is shown in doubled rhombohedral cell. The rhombohedral (shaded) Brillouin zone is shown inside the larger BZ of the fcc unit cell below. The important Eu d overlap with the N p bands occurs at the X point in the large BZ, corresponding to the L point of the small BZ.

compensating holes go into the $2p$ band, at Γ and at the X point. The remaining complete spin polarization of the N $2p$ holes may be important for the $4f$-$4f$ exchange processes (Sec. IV).

The only previous calculations on EuN were by Horne *et al.*[20] using the self-interaction-corrected LDA (SIC-LDA) approach implemented within the linearized muffin-tin orbital band structure code. Horne *et al.* reported only the DOS for FM spin alignment, with the results being significantly different from what we have obtained, as the considerable differences in the methods might suggest. Regarding the Eu $5d$ and N $2p$ bands, they obtained a semiconducting result with a separation of 1.4 eV, whereas LDA+U gives an overlap of several tenths of an eV for FM alignment. Their N $2p$ bandwidth is 15% narrower than the LDA+U value of 4.5 eV. In SIC-LDA the unoccupied majority $4f$ orbital lies at the very bottom of this gap, mixes strongly with the N $2p$ states, acquires a 1 eV width and becomes slightly occupied. The SIC-LDA result thus is a half metal (for FM alignment). The minority $4f$ bands (unoccupied) lie about 4 eV above E_F, quite similar to what we find from LDA+U. The majority $4f$ states in SIC-LDA lie about 12 eV below E_F with 0.5 eV width, whereas those obtained from LDA+U are centered only 5.5 eV below E_F with a 2 eV spread. As we discuss in Sec. III C, the $4f$ state splittings in LDA+U are a result of the anisotropy of the direct and exchange interactions. These differing results generally reflect the distinctive band shifts of the respective methods: SIC-LDA lowers (very strongly) the occupied $4f$ states, whereas LDA+U lowers occupied and raises unoccupied $4f$ states each by some fraction of U determined by the orbital occupancies.

Other rare earth nitrides have been reported in experimental studies to be semimetals[21–23] as our results give for EuN, while the group IIIA mononitrides (BN, AlN, GaN, InN) are known to be wide gap semiconductors. Calculations of the electronic structure of the closely related compound GdN have been given by Petukhov *et al.*,[24] who used an atomic sphere approximation for the potential and treated the $4f$ states corelike (thus removed from the band structure problem). These calculations gave a small (0.1 eV) overlap between the valence band maximum at Γ involving N $2p$ states, and a conduction band minimum at X comprised of strongly Eu $5d$ character. This band structure is very much like what we obtain for EuN (as well as for AFM EuP below). By averaging over the spin splitting (and also surveying the AFM bands) we deduce a semimetallic band overlap of $\sim$0.1 eV for EuN, and $\sim$1.0 eV for EuP, both of which increase under pressure.

B. EuP

The band structures of FM- and AFMII-ordered EuP are shown in Fig. 4. The main features of EuN remain in EuP, specifically the character of the valence and conduction bands and the semimetallic band crossing at the $X(L)$ point. In EuP, the valence P $3p$ bands that determine E_F are higher

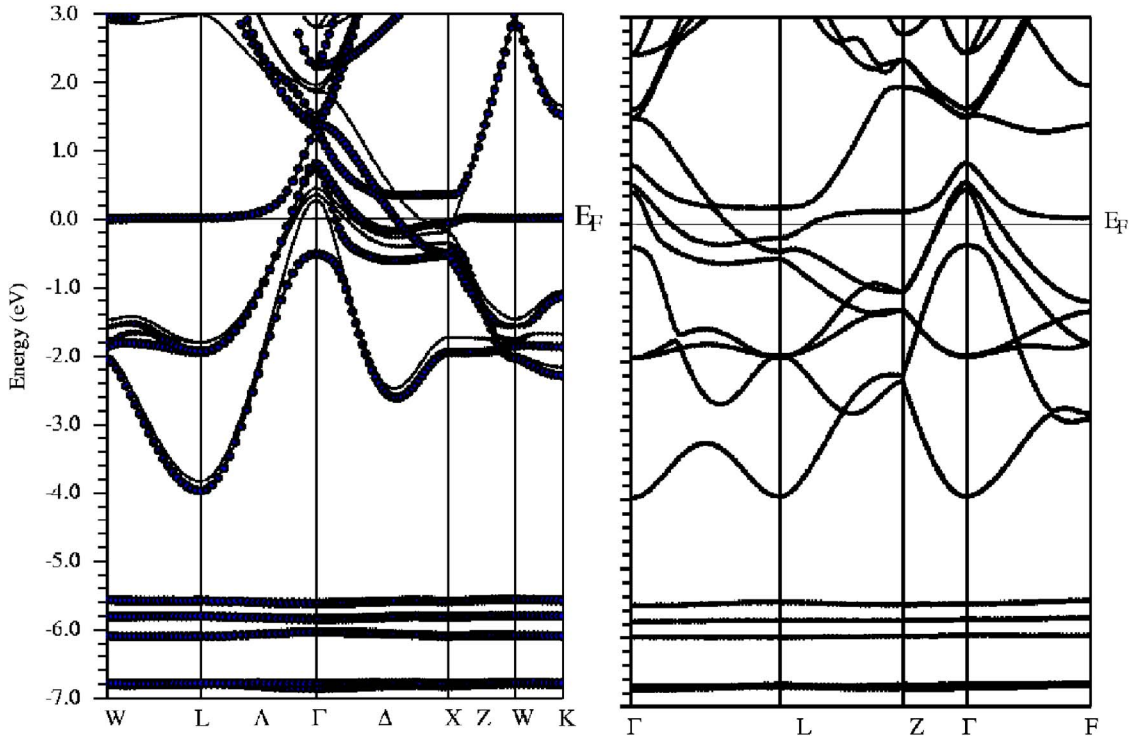

FIG. 4. (Color online) Left panel: bands of FM EuP in the fcc cell with majority spin character highlighted. Right panel: AFM EuP in the rhombohedral cell at equilibrium volume. Note that the $4f$-$3p$ mixing near E_F is so strong in the AFM case that the unoccupied $4f$ band above E_F is not readily obvious.

in energy (relative to the $4f$ bands) than the analogous $2p$ bands in EuN. Conversely, one may adopt the viewpoint that the Eu $5d$ and $4f$ bands are shifted downward relative to the P $3p$ bands (see Fig. 5). One feature clearly relevant to magnetic interactions is $4f$-$3p$ hybridization. The unoccupied majority $4f$ band sits just above E_F and mixes strongly with the P $3p$ band near X along the Γ-X line. Holes in the $3p$ band are consequently near the Γ point only and *not* from the majority spin band near X which is pushed down by hybridization with the f band. In contrast to EuN, EuP with FM alignment is not a half-metal and significantly, the $3p$ holes are only weakly spin polarized.

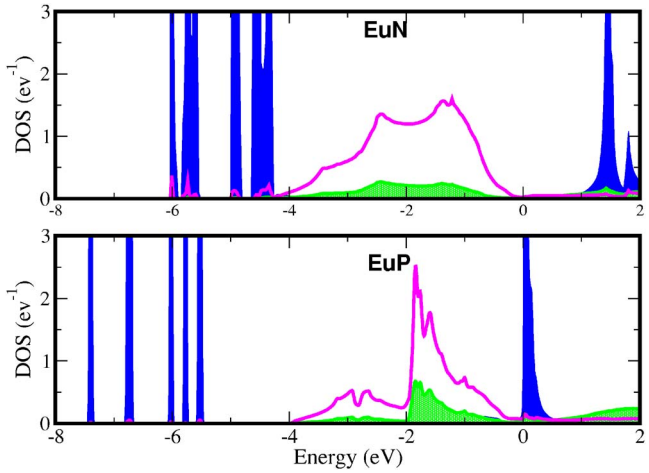

FIG. 5. (Color online) A partial DOS plot for FM EuN and AFM EuP. Top panel: The orbitally resolved $5d$,$4f$ states of Eu and $2p$ states of N at a compression of 12% by volume (15 GPa). The unoccupied $4f$ band is more than 1 eV above the filled N $2p$ bands. The bottom of the valence $5d$ band is filled, providing the mechanism for superexchange. Bottom panel: At equilibrium volume, the unoccupied f band sits immediately above E_F, and the occupied bands are completely separated from the filled P $3p$ bands.

C. $4f$ Occupation and Hund's second rule

It should be understood at the outset that any band picture of the $4f$ states has serious intrinsic limitations that have been recognized for some time and occasionally addressed.[25] A band structure is hoped to represent, in a mean field manner, the electron removal spectrum for occupied states and the electron addition spectrum for unoccupied states. The open $4f$ shell is a highly correlated local system: individual spins are strongly coupled and aligned to form the total spin S, orbital occupations are correlated to give L, and Hund's third rule (SOC) gives the ground state J. In such ions there is a manifold of low energy excitations in which the particle number remains unchanged ($J \neq 0$ multiplets at higher energy). These multiplet excitations, often affected strongly by crystal fields, lie outside the realm of band structures, even in a "zeroth order" description.

Density functional theory (DFT), which gives rise in the process of energy minimization to the Kohn-Sham band structure, is itself a many body theory for the system energy. There have been a few indications that the LDA+U approach is useful in modeling (perhaps predicting) some of these particle-number conserving excitations.[19,26] More specifically, one can ask whether the LDA+U approach is ca-

pable of reproducing Hund's rules, i.e., obtaining the lowest energy for the correct configuration L,S,J. Solovyev *et al.* have addressed this question,[27] and Gotsis and Mazin have obtained encouraging results[28] for some Sm intermetallic compounds.

The separations of the filled flat $4f$ bands in Figs. 2–4 are due to the strong orbital dependence of the exchange interaction, whose full anisotropy is incorporated into the LDA+U code. These differing energy shifts are determined by the Hund's exchange constant J^H. To clarify the origin of the splitting between the f bands, we present an explicit example of the potential matrix elements used in the LDA+U procedure for the case where the density matrix is diagonal $n^{\sigma}_{mm'}=n^{\sigma}_{m}\delta_{mm'}$ (which avoids uninstructive complications that arise in the general case). Then the only matrix elements which enter the LDA+U energy are the direct and exchange integrals of the form

$$\mathcal{U}_{mm'}=\langle mm'|V_{ee}|mm'\rangle,$$

$$\mathcal{J}^{H}_{mm'}=\langle mm'|V_{ee}|m'm\rangle. \quad (1)$$

In the atomic limit these are given simply in terms of the $l=3$ Slater integrals F_0, F_2, F_4, F_6 and angular factors. In the LDA+U method these are represented in terms of two constants "direct" U and "exchange" J^H

$$U=F^0, \quad J^H=(F_2+F_4)/14 \quad (2)$$

and the ratio $F_4/F_2\sim 0.625$, $F_6/F_2\sim 0.494$. With $U=8$ eV and $J^H=1$ eV as we have used, the corresponding Slater integrals are $F_0=8.0$ eV, $F_2=11.92$ eV, $F_4=7.96$ eV, and $F_6=5.89$ eV. (F_0 is strongly screened in the solid so atomic values cannot be used directly.) See Shick *et al.*[18] and references therein for details about how these Slater integrals are used in the LDA+U method.

If J^H is set to zero, these simplify to an isotropic repulsion $\mathcal{U}_{mm'}=F_0$, and to a diagonal and orbital-independent $\mathcal{J}^{\mathcal{H}}{}_{mm'}=F_0\delta_{mm'}$, the latter simply removing the self-interaction. Thus for $J^H=0$ no distinction between different orbitals is made, and filled orbitals will all be shifted downward equally, while unfilled orbitals will be shifted upward equally. An important and unsatisfactory result is that the energy differences based on orbital quantum number m (which give rise to Hund's 2nd rule splittings in the atomic limit) are absent when $J^H=0$.

With $J^H\neq 0$ the diagonal elements become orbital dependent, and each occupied orbital obtains (self-consistently) its own downward shift in energy. To illustrate the strong orbital dependence (anisotropy) we present explicitly the $\mathcal{U}_{mm'}$ and $\mathcal{J}_{mm'}$ matrices for Eu in Appendix A. The resulting differences in eigenenergies can be pronounced, as in Fig. 4 where different occupied $4f$ bands are separated by as much as 2 eV. J^H therefore has two roles: (1) it provides the anisotropy of the direct Coulomb repulsion $\mathcal{U}_{mm'}$ (which is independent of m,m' if $J^H=0$) and (2) it has the more commonly understood aspect of providing the intra-atomic exchange coupling $\mathcal{J}_{mm'}$, $m\neq m'$.

D. Equation of state

We fit the energy vs volume curves for the FM/AFM spin configuration of EuN/EuP to an equation of state:[29]

$$E=a+bV^{-1/3}+cV^{-2/3}+cV^{-1} \quad (3)$$

and extracted the LDA equilibrium constants and bulk moduli. EuN has a calculated equilibrium volume of 406.9 a.u.^{3}, 5% smaller than experiment (consistent with typical LDA error) and a bulk modulus, $B=130$ GPa. The volume of EuP is 612.6 a.u.^{3}, consistent with the larger P^{3-} ion, and again is 5% smaller than experiment. It has a bulk modulus of 86 GPa, making it much softer than EuN. The lattice constants of EuN and EuP have been calculated previously by Horne *et al.*,[20] whose SIC results are very similar to ours.

IV. EXCHANGE ENERGY AND INTERACTIONS

In the rocksalt structure each Eu ion has potential exchange coupling to its twelve nearest Eu neighbors through an intermediate pnictide ion at a 90° angle, and to each of its six second neighbors at a 180° angle. The Goodenough-Kanamori superexchange rules lead one to anticipate a ferromagnetic nearest-neighbor interaction, while the second nearest-neighbor interaction will be antiferromagnetic. These guidelines are based on perturbation expansions appropriate for insulators, and may be misleading here where other mechanisms also arise [Rudermann-Kittel-Kasuya-Yosida (RKKY) interactions through the electron and hole carriers, specifically]. We probe some energetics of the superexchange processes by calculating the energy differences between ferromagnetic and AFMII spin alignments, using the same rhombohedral cell to improve numerical precision. For the experimental lattice constant of EuN, there is a small energy difference $\Delta E=E_{\mathrm{FM}}-E_{\mathrm{AFM}}=-4.9$ meV. ΔE increases in magnitude with compression and reaches a value of -10.1 meV when the lattice parameter is reduced by $\approx 4\%$. In EuP, the energy differences are somewhat larger and of the opposite sign, with $\Delta E=12.8$ meV at equilibrium volume decreasing to $\Delta E=9.2$ meV at a compression by 4% of the lattice constant. The calculated ground state of EuN is therefore FM, while that of EuP is AFM. Our single total energy difference is only sufficient to give a single exchange constant. As can be seen in the equation below, the effective exchange constant (which includes *all* exchange interactions between *all* neighbors) may be attributed solely to the first neighbors or solely to the second neighbors, resulting in an identical expression. Using nearest neighbors only in a classical $S=3$ Heisenberg model gives for the two magnetic states

$$E_{\mathrm{AFM}}=0, \quad E_{\mathrm{FM}}=6KS^2, \quad \Delta E=6KS^2. \quad (4)$$

Using second nearest neighbors only gives

$$E_{\mathrm{AFM}}=-3KS^2, \quad E_{\mathrm{FM}}=3KS^2, \quad \Delta E=6KS^2.$$

Extracting the exchange constant from these formulas gives $K_{\mathrm{EuN}}=-0.09$ meV (1 K) at zero pressure and $K_{\mathrm{EuN}}=-0.19$ meV (2.2 K) at 4% reduced lattice constant or 15 GPa. For EuP, the exchange interaction is somewhat

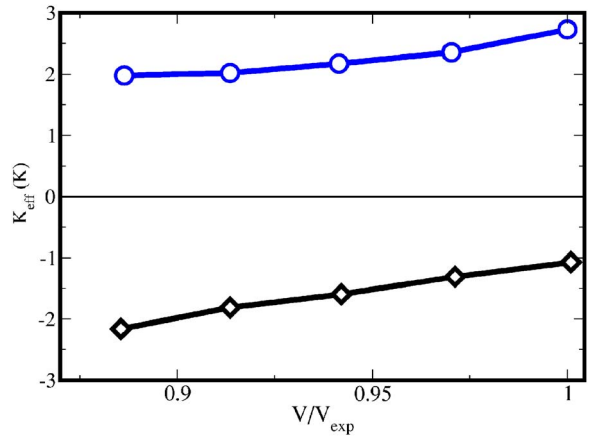

FIG. 6. (Color online) The inferred exchange constant K for EuN and EuP. Top panel: K for EuP is positive (AFM order) and decreases with pressure. In analogy with the $3d$ transition metal monoxides, AFMII order may more likely be due to next-neighbor AFM coupling than to near-neighbor AFM coupling. Lower panel: K for EuN is negative (ferromagnetic order) and increases in magnitude with pressure.

larger, $K_{\mathrm{EuP}}=0.24$ meV (2.8 K) at equilibrium pressure, and opposite in sign. It also has the opposite pressure dependency which, due to the smaller bulk modulus, produces a decrease of nearly 25% in K_{EuP} at a pressure of 7.5 GPa (see Fig. 6). We observe that for the larger compound, EuP, the effective interaction between ions decreases with increasing pressure despite the decreased distance between neighbors, possibly due to decreasing competition from first neighbor exchange. EuN is firmly within the FM regime and pressure has the expected effect of increasing the coupling. Recent pressure studies show that EuN retains the rocksalt structure up to 70 GPa.[30] Assuming that the lattice constant and K maintain a linear relationship at high pressure (Fig. 6 indicates that in reality it is slightly sub-linear), we can extrapolate that $K=0.3$ meV (3.5 K) at 70 GPa. As we will show in the next section, an exchange coupling of this magnitude can have observable effects on the susceptibility. Despite a difference in Eu valency, these results are quite consistent with the trends found for the series of $Eu^{2+}X$ compounds,[12] namely, that compounds with a large lattice constant are AFM, while compounds under high pressure or with smaller lattice constants are FM. The exchange constants of Ref. 12 were resolved into K_1 and K_2 separately, both of which are comparable in magnitude to our single effective K.

V. A TOY MODEL STUDY

Since the states of ions are most readily described in terms of their total angular momentum $\vec{J}_i$ it is natural and customary to use the effective Hamiltonian $K_{eff}\vec{J}_1\cdot\vec{J}_2$ for the coupling. However, the actual exchange interaction proceeds via the spins $\vec{S}_1$ and $\vec{S}_2$, so we begin this investigation by considering the more microscopic model Hamiltonian expressed in terms of $\vec{S}_i$ and $\vec{L}_i$. Our two identical site Hamiltonian $(i=1,2)$ is

$$H = K\mathbf{S}_1\cdot\mathbf{S}_2 + \lambda\sum_i \mathbf{L}_i\cdot\mathbf{S}_i - \sum_i \mathbf{M}_i\cdot\mathbf{B} + \sum_i (\mathbf{D}\cdot\mathbf{L}_i)^2. \quad (5)$$

This Hamiltonian includes the interactions we expect to be important in the investigation of magnetic behavior in EuN or EuP (although interactions may extend to more neighbors). We choose the spin-orbit constant to be $\lambda=323$ cm^{-1}=40 meV, a typical value for the $^7F_0\rightarrow{}^7F_1$ transition observed by spectroscopic[8,31–33] measurements on several Eu^{3+} compounds. The exchange parameter K will be varied to examine the macroscopic effects of the exchange coupling, with the physically relevant values taken from our LDA+U calculations. The most conservative estimate is obtained by directly importing the K derived by mapping energy differences onto the Heisenberg model. This gives an upper bound of $K/\lambda\sim 0.01$ for EuN (under high pressure) and for EuP at equilibrium volume. It may be more realistic to establish K by directly forcing the toy model to reproduce the density functional AFM-FM energy differences (per Eu ion pair). This gives a much higher value ratio of K/λ: 0.21 for EuP and 0.08 for EuN, both at their respective equilibrium volumes. The single-ion anisotropy $\vec{D}$ is taken to be of similar magnitude (2 meV), with the easy axis defining the $\hat{z}$ axis.

Our basis includes $J=0$ and three $J=1$ states on each of the two sites. The next J multiplet $^7F_2$ is $2\lambda\sim 900$ K higher in energy than $^7F_1$, so it will not contribute to the low-energy regime we explore. This basis of four states per site leads to a 16×16 Hamiltonian matrix. Matrix elements are readily evaluated in the $|L,L_z;S,S_z\rangle$ basis; the expansion of the states $|J,J_z\rangle$ states $(\vec{J}=\vec{J}_1+\vec{J}_2)$ in the $|L,L_z;S,S_z\rangle$ states is given in Appendix B.

For $K=0$, $D=0$, Hund's rules give the $J_i=0$ ground state on each site (and trivially $J_{\mathrm{tot}}=0$). As discussed in the Introduction, any projection of each magnetic moment $\vec{M}_i=\mu_B(L_i+2\vec{S}_i)$, and therefore the total $\vec{M}=\vec{M}_1+\vec{M}_2$, vanishes for uncoupled spherical ions although its mean square value is large. Exchange coupling K introduces mixing between the states of the two sites, but preserves the spin rotational symmetry of the Hamiltonian. Expectation values of both individual and total magnetic moments (and individual angular momenta) therefore are zero, but correlation functions such as $\langle\vec{S}_1\cdot\vec{S}_2\rangle$ and $\langle\vec{M}_1\cdot\vec{M}_2\rangle$ grow as the strength of the coupling grows. Single-site anisotropy $\vec{D}\neq 0$ or field $\vec{B}$ destroys the rotational symmetry of H and introduces additional mixing of states.

Figure 7 shows the increase of the spin-spin and magnetic moment correlation functions in the ground state as K increases. In the limit $K/\lambda\rightarrow\infty$, the model reduces to a two site Heisenberg model, with a well known analytic solution $\vec{S}_1\cdot\vec{S}_2=(S^2-S_1^2-S_2^2)/2=-12$, where $S=0$ in the ground state and $S_i=L_i=3$. The restricted basis set we use does not span the entire Hilbert space of the Heisenberg Hamiltonian and the spin-spin correlation function therefore asymptotes to a smaller value of −7.18. The higher J multiplets necessary for $\langle\vec{S}_1\cdot\vec{S}_2\rangle$ to attain the analytical ground state value are moved too high in energy by the scale of the spin-orbit parameter, therefore −7.18 should be considered the maximum anti-

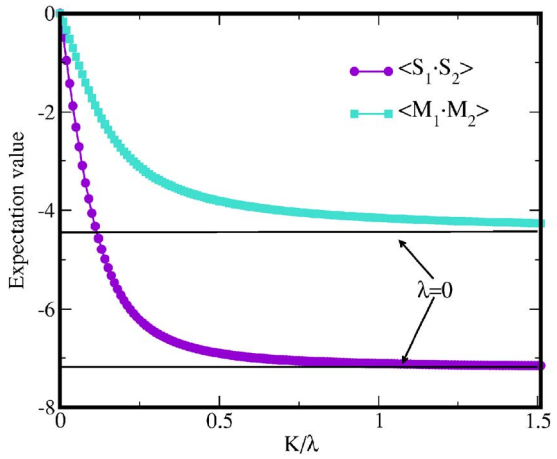

FIG. 7. (Color online) Alignment of spins and magnetic moment as a function of K/λ. The horizontal line in each case marks the value of maximum possible alignment possible in the restricted Hilbert space of the model.

alignment of spins within this system. The asymptotic and analytically calculated expressions for $\langle \mathbf{M}_1 \cdot \mathbf{M}_2 \rangle$ are also different because of the restricted basis set.

For small K the order parameter grows linearly with K with steep slope, and at $K/\lambda = 0.175$, $\langle \vec{S}_1 \cdot \vec{S}_2 \rangle$ reaches half its maximum value, as shown in Fig. 7. A similar conclusion holds for the moment-moment correlation function. Rotational symmetry of the system is broken, allowing a nonzero moment and ready detection, by single-ion anisotropy $\vec{D} \neq 0$ or by application of a magnetic field $\vec{B}$.

A calculation of $\langle M_{\|} \rangle$ vs B in thermal equilibrium, presented in Fig. 8, shows two clear crossovers at fields of ~720 and 1450 T. These transitions exist only for relatively high values of K and low temperatures and correspond to qualitative changes in eigenvectors as the external B field overcomes the exchange and spin-orbit energies, respectively. At higher temperatures or lower K/λ, every state in

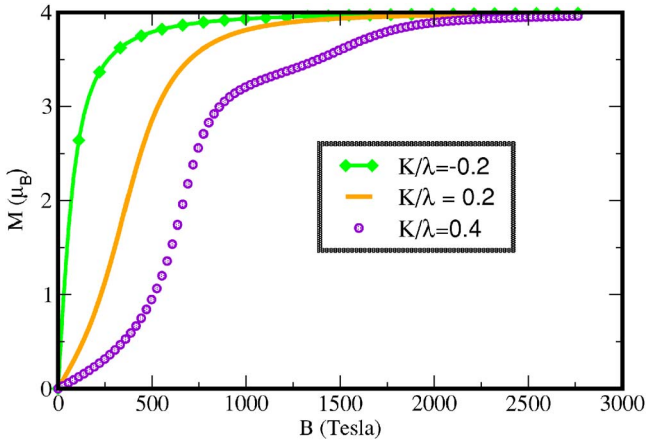

FIG. 8. (Color online) Magnetic moment vs applied magnetic field for a thermodynamic ensemble of two site "molecules" described by Eq. (5). The curves are sensitive to the value of the exchange constant K, suggesting that this quantity can be probed with experimental measurements of M vs B.

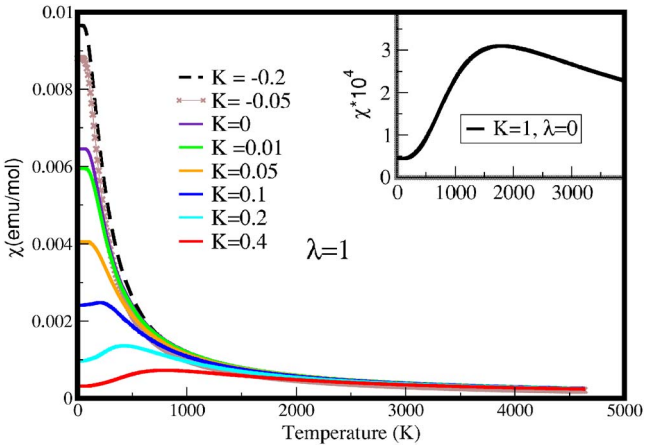

FIG. 9. (Color online) The magnetic susceptibility of the two-site model with various levels of spin-spin interaction. The curve resembles a Van Vleck paramagnetic susceptibility for small K, and smoothly evolves to a shape of susceptibility typical of local AFM correlations when K dominates.

the Hilbert space is present even in the ground state and the curve evolves smoothly. Because fields of this magnitude are experimentally unattainable and would be strong enough to mix in even higher J multiplets ($J=2,3,\ldots$), only the low field part of the curve in Fig. 8 can be taken seriously. In low fields, $\langle M \rangle$ is linear in B with a slope (susceptibility χ) that is strongly dependent on the exchange coupling. This sensitivity suggests that the degree of spin-spin correlation in a system containing Eu^{3+} ions can be probed by examining the temperature dependence of the magnetic susceptibility.

Figure 9 shows the calculated $\chi(T;K,\lambda)$ curves for different values of K within our two site model. For small K, the curves show typical Van Vleck paramagnetic behavior,[34] characterized by an initial flat region which quickly decreases towards zero after a certain onset temperature. The magnitude of the susceptibility in the constant region of the curve and the onset temperature of the decrease are both extremely sensitive to the K/λ ratio. Susceptibility curves reported in Refs. 7–10 for Eu^{3+} compounds are very similar to those calculated within our model for small K. For larger values of K, beginning with $K/\lambda \sim 0.1$, the curve begins to develop a maximum at non-zero temperature which then evolves, with growing K, more toward a standard AFM susceptibility as shown in the inset of Fig. 9 for the limit $K/\lambda \rightarrow \infty$. Since the K/λ ratio is manipulable by pressure, the effect of increasing K (signalling increasing spin-spin correlation) should be observable in the susceptibility curve, even for the conservative estimates of K/λ mentioned earlier.

The first-principles calculation indicates that a non-zero spin-spin interaction of conventional strength does indeed exist. Though the energy difference between spin orientations for EuN is small at ambient volume, its magnitude can be increased with pressure. For EuP, the energy difference is largest at equilibrium volume and is sensitive to manipulation by pressure. The model calculation shows that any non-zero interaction results in nonvanishing spin correlation $\langle \vec{S}_i \cdot \vec{S}_j \rangle$.

VI. DISCUSSION

We have initiated the study of the electronic structure of EuN and EuP specifically, and of the spin coupling and resulting behavior of the $4f^6$ ion more generally. The strong spin polarization of the $4f$ shell, and the coupling of the moments $L+S=J=0$ to produce a nonmagnetic ion, makes a prediction of the physical electronic structure somewhat uncertain. We obtain, however, that both EuN and EuP are semimetallic due to overlap of the valence pnictide p bands with the conduction Eu $5d$ bands. Recent measurements of the resistivity of pressed powders of EuN show a positive temperature coefficient, i.e., metallic or semimetallic conduction.[35]

We point out that even though the expectation value of any (vector) spin may be zero, exchange coupling will give rise to nonvanishing spin-spin correlations between coupled ions. This coupling may lead to an unconventional phase transition in which the spin correlation length diverges but there is little or no signal in the magnetic properties. The determination of the ordering temperature acquires new aspects: since entropy is (nearly) absent in both ordered and disordered states, a different mechanism from simple energy-entropy balance may control the ordering temperature. One possibility is that spin-phonon interactions promote disorder: raising the temperature increases thermal vibrations, which modulates the interatomic separations and hence modulates the exchange couplings dynamically. The phase transition would occur at a critical value of the exchange coupling "disorder."

There are other Eu rocksalt compounds (divalent, $4f^7$) with FM ordering, as well as those with AFM ordering. In some cases, such as EuSe, a transition between the two magnetic alignments can be driven by manipulating the U parameter[12] or by applying pressure. Based on our LDA+U results, a state in which the spin moments of Eu ions are antiferromagnetically correlated is unlikely for EuN but probable for EuP. For EuN, a hidden ferromagnetic correlation, or ordering, of spins (accompanied by an identical, but oppositely pointed arrangement of orbital moments) is energetically favored. It could be an experimental challenge to see the hidden "ferromagnetic order," which does not break any crystal symmetry.

ACKNOWLEDGMENTS

The authors are indebted to A. B. Shick for many discussions on this work and for the code to produce the data presented in Appendix A. We acknowledge discussions with Z. Fisk, J. Lynn, S. M. Kauzlarich, J. Kuneš, I. I. Mazin, D. A. Papaconstantopoulos, P. Novak, and D. J. Singh. W.E.P. was supported by DOE Grant No. DE-FG03-01ER45876, DOE's Computational Materials Science Network, and the SSAAP program at LLNL under Grant No. DE-FG03-03NA00071. Research at NRL is supported by the Office of Naval Research.

APPENDIX A

With U=8 eV and $J^H=1$ eV as used in our LDA+U calculations, the direct and exchange matrix elements for diagonal occupation numbers are given by the following tables (the matrix elements are ordered from $l_z=-3\rightarrow l_z=3$ from left to right and up to down):

$$\mathcal{U}_{mm'}=\begin{bmatrix} 9.4 & 7.8 & 7.2 & 7.1 & 7.2 & 7.8 & 9.4 \\ 7.8 & 8.4 & 7.9 & 7.8 & 7.9 & 8.4 & 7.8 \\ 7.2 & 7.9 & 8.7 & 8.4 & 8.7 & 7.9 & 7.2 \\ 7.1 & 7.8 & 8.4 & 9.4 & 8.4 & 7.8 & 7.1 \\ 7.2 & 7.9 & 8.7 & 8.4 & 8.7 & 7.9 & 7.2 \\ 7.8 & 8.4 & 7.9 & 7.8 & 7.9 & 8.4 & 7.8 \\ 9.4 & 7.8 & 7.2 & 7.1 & 7.2 & 7.8 & 9.4 \end{bmatrix},$$

$$\mathcal{J}^H_{mm'}=\begin{bmatrix} 9.4 & 1.55 & 0.95 & 0.53 & 0.48 & 0.37 & 0.74 \\ 1.55 & 8.4 & 1.11 & 1.26 & 0.41 & 0.92 & 0.37 \\ 0.95 & 1.11 & 8.7 & 0.50 & 1.90 & 0.41 & 0.48 \\ 0.53 & 1.26 & 0.50 & 9.4 & 0.50 & 1.26 & 0.53 \\ 0.48 & 0.41 & 1.90 & 0.50 & 8.7 & 1.11 & 0.95 \\ 0.37 & 0.92 & 0.41 & 1.26 & 1.11 & 8.4 & 1.56 \\ 0.74 & 0.37 & 0.48 & 0.53 & 0.95 & 1.55 & 9.4 \end{bmatrix}.$$

APPENDIX B

We give here the parentage of the $|J,J_z\rangle$ states in terms of the product states $|S,S_z;L,L_z\rangle\equiv|S_z,L_z\rangle$ ($S=3$, $L=3$ are fixed). For our considerations only the $J=0$ and $J=1$ states are needed.

$$|0,0\rangle=\frac{1}{\sqrt{7}}[(-3,3\rangle-|-2,2\rangle+|-1,1\rangle-|0,0\rangle+|1,-1\rangle-|2,-2\rangle+|3,-3\rangle],$$

$$|1,-1\rangle=\frac{1}{2\sqrt{7}}[\sqrt{3}|2,-3\rangle-\sqrt{5}|1,-2\rangle+\sqrt{6}|0,-1\rangle-\sqrt{6}|-1,0\rangle+\sqrt{5}|-2,1\rangle-\sqrt{3}|-3,2\rangle],$$

$$|1,0\rangle=\frac{1}{2\sqrt{7}}[-3|-3,3\rangle+2|-2,2\rangle-|-1,1\rangle+|1,-1\rangle-2|2,-2\rangle+3|3,-3\rangle],$$

$$|1,1\rangle=\frac{1}{2\sqrt{7}}[\sqrt{3}|3,-2\rangle-\sqrt{5}|2,-1\rangle+\sqrt{6}|1,0\rangle-\sqrt{6}|0,1\rangle+\sqrt{5}|-1,2\rangle-\sqrt{3}|-2,3\rangle].$$

[1] W. Klemm and G. Winkelman, Z. Anorg. Allg. Chem. **288**, 87 (1956).
[2] J. Kordis and K. A. Gingerich, J. Am. Helicopter Soc. **56**, 581 (1973).
[3] R. C. Brown and N. J. Clark, J. Inorg. Nucl. Chem. **36**, 2507 (1974).
[4] H. Jacobs and U. Fink, Z. Anorg. Allg. Chem. **438**, 151 (1978).
[5] R. Didchenko and F. P. Gortsema, J. Phys. Chem. Solids **24**, 863 (1963).
[6] S. P. Gordienko and K. E. Mironov, Izv. Akad. Nauk SSSR, Neorg. Mater. **19**, 151 (1983).
[7] K. Tezuka, Y. Hinatsu, N. Masaki, and M. Saeki, J. Solid State Chem. **138**, 342 (1998).
[8] C. K. Jayasankar, E. Antic-Fidancev, M. Lemaitre Blaise, and P. Porcher, Phys. Status Solidi B **133**, 345 (1985).
[9] B. Antic, M. Mitric, and D. Rodic, J. Phys.: Condens. Matter **9**, 365 (1997).
[10] S. Kern, P. M. Raccah, and A. Tveten, J. Phys. Chem. Solids **31**, 2639 (1970).
[11] J. Kuneš and W. E. Pickett, Phys. Rev. B **69**, 165111 (2004).
[12] J. Kuneš and W. E. Pickett, J. Phys. Soc. Jpn. **74**, 1408 (2005).
[13] P. Blaha, K. Schwarz, G. K. H. Madsen, D. Kvasnicka, and J. Luitz, WIEN2K, 2002, an Augmented Plane Wave + Local Orbitals Program for Calculating Crystal Properties (Karlheinz Schwarz, Technische Universitat Wien, Austria).
[14] J. P. Perdew and Y. Wang, Phys. Rev. B **45**, 13244 (1992).
[15] V. I. Anisimov, J. Zaanen, and O. K. Andersen, Phys. Rev. B **44**, 943 (1991).
[16] V. I. Anisimov, I. V. Solovyev, M. A. Korotin, M. T. Czyzyk, and G. A. Sawatzky, Phys. Rev. B **48**, 16929 (1993).
[17] A. G. Petukhov, I. I. Mazin, L. Chioncel, and A. I. Lichtenstein, Phys. Rev. B **67**, 153106 (2003).
[18] A. B. Shick, A. I. Liechtenstein, and W. E. Pickett, Phys. Rev. B **60**, 10763 (1999).
[19] A. B. Shick, W. E. Pickett, and A. I. Liechtenstein, J. Electron Spectrosc. Relat. Phenom. **114-116**, 753 (2001).
[20] M. Horne, P. Strange, W. M. Temmerman, Z. Szotek, A. Svane, and H. Winter, J. Phys.: Condens. Matter **16**, 5061 (2004).
[21] G. Travaglini, F. Marabelli, R. Monnier, E. Kaldis, and P. Wachter, Phys. Rev. B **34**, 3876 (1986).
[22] P. Wachter and E. Kaldis, Solid State Commun. **34**, 241 (1980).
[23] L. Degiorgi, W. Bacsa, and P. Wachter, Phys. Rev. B **42**, 530 (1990).
[24] A. G. Petukhov, W. R. L. Lambrecht, and B. Segall, Phys. Rev. B **53**, 4324 (1996).
[25] U. von Barth, Phys. Rev. A **20**, 1693 (1979).
[26] A. B. Shick, V. Janis, V. Drchal, and W. E. Pickett, Phys. Rev. B **70**, 134506 (2004).
[27] I. V. Solovyev, A. I. Liechtenstein, and K. Terakura, Phys. Rev. Lett. **80**, 5758 (1998).
[28] H. J. Gotsis and I. I. Mazin, Phys. Rev. B **68**, 224427 (2003).
[29] D. M. Teter, G. V. Gibbs, M. B. Boisen, D. C. Allan, and M. P. Teter, Phys. Rev. B **52**, 8064 (1995).
[30] B. Maddox and C. S. Yoo (private communication).
[31] J. R. G. Thorne, M. Jones, C. S. McCaw, K. M. Murdoch, R. G. Denning, and N. M. Khaidukov, J. Phys.: Condens. Matter **11**, 7851 (1999).
[32] C. Gorller-Walrand, K. Binnemans, and L. Fluyt, J. Phys.: Condens. Matter **5**, 8359 (1993).
[33] X. Y. Chen and G. K. Liu, J. Solid State Chem. **178**, 419 (2005).
[34] J. H. Van Vleck, *The Theory of Electric and Magnetic Susceptibilities* (Oxford University Press, London, 1965).
[35] M. S. Bailey, J. Hunting, and F. J. DiSalvo (private communication).